

Run-and-tumble particles in slit geometry as a splitting probability problem

Derek Frydel

Department of Chemistry, Universidad Técnica Federico Santa María, Campus San Joaquín, Santiago, Chile

(Dated: October 10, 2024)

Run-and-tumble particles confined between two walls seem like a simple enough problem to possess analytical tractability. Yet up to date no satisfactory analysis is available for dimensions higher than one. This work contributes to the theoretical understanding of this system by reinterpreting it as a splitting probability problem. Such reinterpretation permits us to formulate the problem as the integral equation, rather than a more standard differential equation based on the Fokker-Planck equation. In addition to providing an analogy with another phenomenon, the reinterpretation permits a new type of analysis, yields useful results, and offers some analytical tractability.

I. INTRODUCTION

The opening sentence of Anna Karenina states: "All happy families are alike; each unhappy family is unhappy in its own way." This sounds a bit like statistical mechanics if we substitute happiness with equilibrium and unhappiness with non-equilibrium. Each non-equilibrium system "is unhappy in its own way."

Anyone working even with the most idealized non-equilibrium systems might have recognized that a slight modification can bring about significant changes. Not just changes of physical properties but changes that require very different tools of analysis. For example, solving the problem of active particles in a harmonic trap is not particularly helpful when trying to analyze the system of particles confined between two walls. Changing interest from one system to another feels like one has to start the learning process all over again. This is frustrating but also makes non-equilibrium statistical mechanics interesting.

Run-and-tumble particle model (RTP) is probably the most ideal system of active particles and it could be regarded as an ideal-gas-model of active matter. It has all the features of an active particle implemented in the most straightforward way. Yet even for the simplest of confinements, the resulting theoretical problem can be overwhelming.

A typical starting point of theoretical analysis is the Fokker-Planck equation, which in most cases cannot be solved exactly. One can assume that by formulating the problem in terms of a marginal stationary distribution with a reduced number of variables some complexity can be reduced. The difficulty with this idea is that it is not clear how to arrive at such a formulation. There is no direct path from the Fokker-Planck equation to such an alternative formulation.

For RTP particles in a harmonic trap in two-dimensions it was possible to obtain a third order-differential equation for a stationary marginal distribution [1] by analyzing the moments of a marginal distribution [2, 3]. The same trick no longer works when applied to slit geometry. One of the features of slit geometry is that a fraction of particles remains adsorbed onto a wall. This leads to singularities at the location of a wall, making mathematics complicated. Thus, despite its simplicity, the system of RTP particles between two walls in a stationary state remains an unsolved problem.

This article is an attempt to rectify this situation. To do this,

we reinterpret RTP particles between two walls in a stationary state as the splitting probability problem [4–8], where the splitting probability is the probability that a random walker, initially at some location in the region between the two walls, reaches the wall on the right-hand-side without reaching first the wall on the left-hand-side. We arrive at this alternative description by modifying the microscopic motion of particles: rather than using a continuous time Langevin dynamics, our particles move by discontinuous jumps. Although different on the microscopic level, on the macroscopic level the two systems are identical. This permits us to choose the macroscopic framework that is more convenient — in this case the framework based on discontinuous jumps and represented by an integral equation.

Other phenomena that exhibit the splitting probability behavior are the melting probability of a heteropolymer [9], the fixation probability of a mutant in population dynamics [10], and transmission probability of photons or neutrons through a slab of a scattering medium [11–13]

The RTP model was originally conceived to represent the motion of bacteria [14, 15]. RTP particle moves at a constant velocity but randomly changing orientation. Orientations change at time intervals drawn from an exponential distribution. For a system in one-dimension, there are two possible orientations, which simplifies mathematics and allows for exact results. An extensive analysis of the RTP model in one-dimension has been done in [16]. The entropy production rate of the one-dimensional system was studied in [17–19]. Dynamic properties, including first passage, survival probability, and local time were studied in [20–23]. Extensions of the RTP model in one-dimension to include more than two swimming velocities have been considered in [24–27]. RTP particles in a harmonic potential in one-dimension have been investigated in [1, 3, 24, 28–32]. RTP particles in other types of potentials and under different conditions has been considered in [33–43]. Recently, effective diffusion of RTP particles in a slit geometry has been investigated in [44].

II. THE MODEL

The run-and-tumble dynamics consists of two stages. During the "run" stage a particle moves with the swimming velocity $\mathbf{v} = v_0 \mathbf{u}$, where v_0 is the constant magnitude and \mathbf{u} is the unit vector designating the direction of motion. During the

"tumble" stage, which occurs instantaneously, the unit vector \mathbf{u} changes to any other orientation with uniform probability. The time t_p during which a velocity persists in a given orientation is drawn from an exponential distribution

$$p_t = \frac{e^{-t_p/\tau}}{\tau}, \quad (1)$$

where $\tau = \langle t \rangle$ is the average persistence time during which a swimming velocity persists in a given direction.

In the absence of an external potential, the Fokker-Planck equation for RTP particles (for convenience given in 2D) is

$$\dot{n} = -v_0 \mathbf{u} \cdot \nabla n - \frac{1}{\tau} \left(n - \int_0^{2\pi} \frac{d\theta}{2\pi} n \right), \quad (2)$$

where $n \equiv n(\mathbf{r}, \theta, t)$ is the time dependent distribution. Orientation of a swimming motion in 2D is given by $\mathbf{u} = (\cos \theta, \sin \theta)$, where it depends on an angle $\theta \in [0, 2\pi]$. For particles confined between two parallel walls at $x = 0$ and $x = L$, the stationary state is governed by a one-dimensional Fokker-Planck equation,

$$0 = -v_0 \cos \theta n' - \frac{1}{\tau} \left(n - \int_0^{2\pi} \frac{d\theta}{2\pi} n \right), \quad (3)$$

where $v_0 \cos \theta$ is the projection of a velocity vector on the x -axis. The above equation can be written as

$$0 = -vn' - \frac{1}{\tau} \left(n - \int_{-v_0}^{v_0} dv p_v n \right), \quad (4)$$

where $n \equiv n(x, v)$, $v \equiv v_0 \cos \theta$ is the projection of the swimming velocity onto the x -axis (the direction perpendicular to the walls) and $p_v(v)$ is the probability distribution of those velocities. The interaction with the walls is incorporated via the boundary conditions $0 = vn(0, v) = vn(L, v)$, implying zero flux at the walls.

The advantage of Eq. (4) is that it applies to any dimension d , unlike Eq. (3) that is specific to $d = 2$. The dependence on d enters through the probability distribution p_v ,

$$p_v = \frac{1}{2} \begin{cases} \delta(v - v_0) + \delta(v + v_0), & \text{for } d = 1, \\ \frac{2}{\pi} \frac{1}{\sqrt{v_0^2 - v^2}}, & \text{for } d = 2, \\ \frac{1}{v_0}, & \text{for } d = 3, \end{cases} \quad (5)$$

For $d = 1$, two possible swimming directions are $v = \pm v_0$ [17]. For $d = 2$ and $d = 3$, p_v is calculated using the variable change $v = v_0 \cos \theta$,

$$\int_0^{2\pi} d\theta \rightarrow \int_{-v_0}^{v_0} dv \frac{1}{\sqrt{v_0^2 - v^2}},$$

and

$$\int_0^{2\pi} d\phi \int_0^\pi d\theta \sin \theta \rightarrow \int_{-v_0}^{v_0} dv.$$

Within the formalism of Eq. (4), the marginal distribution is defined as

$$\rho(x) = \int_{-v_0}^{v_0} dv p_v(v) n(x, v). \quad (6)$$

One difficulty in dealing with Eq. (4) comes from the interaction with the walls, which leads to "dynamic" adsorption of particles. It is not an adsorption in a usual sense (since walls do not have any attractive potential), but a result of a combined effect of the persistence time and overdamped dynamics. Once an active particle comes in contact with a wall, it does not bounce from it but continues pushing against it, becoming effectively adsorbed and exerting pressure [45–47]. This could be handled by introducing sinks and sources in the Fokker-Planck equation, and such approach was used for the case of active Brownian particles [48, 49], an alternative model of active particles wherein orientation of a swimming velocity changes by diffusion. The resulting mathematics, however, is rather complex. To our knowledge, no similar study has been done for RTP particles between two walls for an arbitrary dimension.

III. REDEFINING THE MICROSCOPIC PROCESS

The usual way to simulate RTP motion is by integrating the Langevin equation which, in the absence of an external potential and using the Euler method, amounts to the following formula

$$x(t + \Delta t) = x(t) + v\Delta t, \quad (7)$$

where the velocity v is drawn from the distribution p_v , given in Eq. (5), at time intervals t_p drawn from p_t in Eq. (1).

If the objective is to study dynamics, then the integration of a Langevin equation is the only option to simulate the system. But if the interest is in a stationary state, then we might have some flexibility in how to sample different configurations.

In this section we propose an alternative microscopic process that yields the same stationary distribution as that generated by the RTP motion. Rather than tracing the position of a particle at each moment, we consider an algorithm that generates configurations at the "tumble" stage and ignores configurations generated during the "run" stage. As a result, rather than moving continuously, a particle appears to be jumping from one place to another.

If at a given "tumble" stage, occurring at time t , a particle is located at $x(t)$, then its position at the subsequent "tumble" stage is

$$x(t + t_p) = x(t) + vt_p. \quad (8)$$

A particle makes a jump of length $\Delta x = vt_p$, where Δx is a product of two random variables v and t_p . Note that the sequential jumps do not correspond to the passage of time of the original RTP system. t_p in this algorithm is just a random parameter used to generate a next jump.

To get rid of any appearance of time, we represent Eq. (8) as

$$x_{n+1} = x_n + vt_p, \quad (9)$$

where x_n is a position of a particle at step n . We refer to the algorithm based on Eq. (9) as the "jump-process" algorithm.

In Fig. (1) we compare stationary distributions generated by the Langevin dynamics of Eq. (7) with stationary distributions generated using the "jump-process" algorithm of Eq. (9) for different values of λ defined as

$$\lambda = \frac{L}{\tau v_0},$$

and for different dimension d . Distributions (correspond-

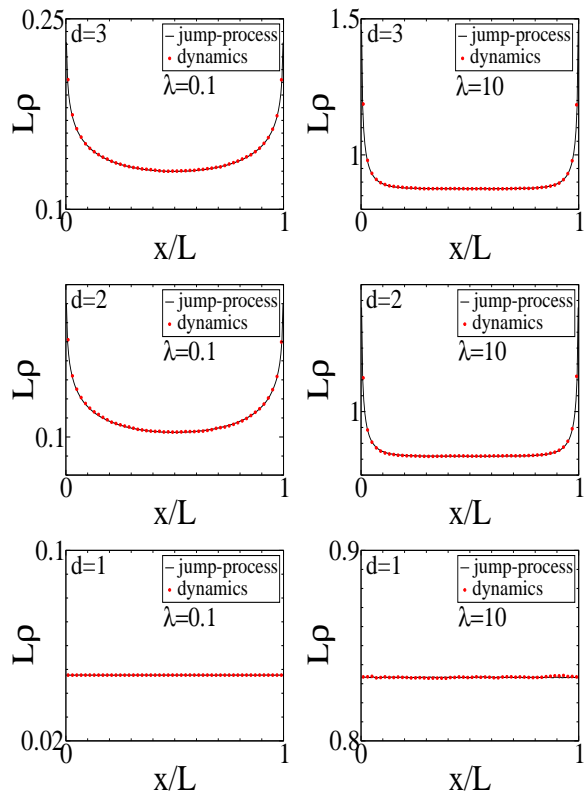


FIG. 1. Stationary (marginal) distributions of RTP particles confined between two walls at $x = 0$ and $x = L$, for different dimension d and $\lambda = \frac{L}{\tau v_0}$. Each distribution is generated by two sampling algorithms. Distributions ρ represent non-adsorbed particles only.

ing to the same physical parameters) generated by different sampling methods are indistinguishable apart from statistical error, confirming the correctness of the "jump-process" algorithm. Apparently, by eliminating the "run" stage of the motion, we do not alter statistical weight of different configurations.

In both algorithms, the interaction with the walls is implemented as follows. Every time a particle crosses one of the walls at $x = 0$ or $x = L$, it is moved to the location of the wall it just crossed. This particle is considered to be adsorbed. If an adsorbed particle crosses a wall at the next step, it is brought back to the location of a wall, thus, it remains adsorbed. The procedure is repeated until a particle moves into the region $x \in (0, L)$, in which case it is considered as de-adsorbed.

Since in a stationary state there is always a fraction of particles that is adsorbed, distributions in Fig. (1) do not integrate to one but $\int_0^L dx \rho(x) = 1 - f_A$ where f_A is the fraction of adsorbed particles, and the distribution of adsorbed particles is represented by two delta functions at the location of the walls,

$$\rho_A = \frac{f_A}{2} \delta(x) + \frac{f_A}{2} \delta(x-L). \quad (10)$$

It is helpful to think of particles as those that are adsorbed and those that are free, as each type exhibits different behavior, for example, they dissipate heat differently. In addition, adsorbed particles are responsible for exerting pressure by pushing against the walls.

Fig. (1) illustrates how stationary distributions vary with dimension. For $d = 1$, all distributions are uniform and the only quantity that changes with λ is f_A and the system for this dimension is fully analytically tractable [16, 17]. The structure of ρ for higher dimensions is more complex. One distinct feature is the emergence of divergences at the location of the walls.

IV. ANALYSIS OF JUMP-PROCESS ALGORITHM

Given a length of a single jump (that depends on two independent random variables t_p and v)

$$\Delta x = vt_p, \quad (11)$$

the probability distribution of jump lengths is defined as

$$G(\Delta x) = \int_0^\infty dt_p p_t(t_p) \int_{-v_0}^{v_0} dv p_v(v) \delta(\Delta x - vt_p). \quad (12)$$

The integral in Eq. (12) is easily evaluated due to the presence of a delta function which eliminates one of the integrals. The evaluated expression depends on a system dimension via p_v in Eq. (5). This leads to three different probability distributions given by

$$G(\Delta x) = \frac{1}{2} \frac{1}{\tau v_0} \begin{cases} e^{-|\Delta x|/\tau v_0}, & \text{for } d = 1, \\ \frac{2}{\pi} K_0(|\Delta x|/\tau v_0), & \text{for } d = 2, \\ \Gamma(0, |\Delta x|/\tau v_0), & \text{for } d = 3, \end{cases} \quad (13)$$

where $K_n(x)$ is the modified Bessel function of the second kind and $\Gamma(n, x)$ is the incomplete gamma function. The distributions for $d = 2$ and $d = 3$ diverges at $\Delta x = 0$. In both cases the singularity is logarithmic,

$$\begin{aligned} K_0 &\sim -\ln \frac{|\Delta x|}{2\tau v_0} - \gamma \\ G_0 &\sim -\ln \frac{|\Delta x|}{\tau v_0} - \gamma, \end{aligned} \quad (14)$$

where γ is the Euler's constant. Divergence for $d > 1$ can be explained by the fact that p_v in those cases does not vanish at $v = 0$. This increases the probability for a particle not to move

at the next jump. A logarithmic divergence is integrable and the second moment of $G(\Delta x)$ exists and is given by

$$\langle \Delta x^2 \rangle = \frac{2\tau^2 v_0^2}{d}. \quad (15)$$

According to this result, the variance decreases with increasing dimension.

V. STATIONARY DISTRIBUTION FROM $G(\Delta x)$

Once we have the exact expression for the probability distribution of jumps, we can calculate a stationary distribution of non-adsorbed particles from the following integral equation:

$$\begin{aligned} \rho(x) = & \int_0^L dx' \rho(x') G(x' - x) \\ & + \frac{f_A}{2} G(x) + \frac{f_A}{2} G(x - L). \end{aligned} \quad (16)$$

The last two terms are contributions of recently de-adsorbed particles, where the factor $f_A/2$ is the fraction of particles adsorbed onto a single wall. Because ρ in Eq. (16) does not include adsorbed particles, it is normalized as

$$\int_0^L dx \rho = 1 - f_A. \quad (17)$$

Even without solving Eq. (16), we can already extract useful results from it. For example, a divergence at each wall for $d > 1$, seen in Fig. (1), can be linked to distributions G in the second line of Eq. (16) and representing the distribution of recently re-adsorbed particles. To confirm that the divergence comes only from those terms, in Fig. (2) we plot the contributions $\rho_I = \int_0^L dx_0 \rho(x_0) G(x - x_0)$ and $\rho_{II} = \frac{f_A}{2} G(x) + \frac{f_A}{2} G(x - L)$, such that $\rho = \rho_I + \rho_{II}$. To plot ρ_{II} , we need to calculate f_A , which is obtained from a "jump-process" simulation. To calculate ρ_I , we use a "jump-process" algorithm in which we ignore particle positions of recently de-adsorbed particles, since these configurations contribute to ρ_{II} .

Regardless of a system dimension, all distributions ρ_I exhibit depletion near the two walls. The depletion arises since walls act like an adsorbing boundary. Since ρ_I does not diverge anywhere in the region $x \in [0, L]$, we conclude that a divergence comes from G at the location of the two walls, and whose exact expression is given in Eq. (13).

For the case of an exponential distribution G , corresponding to $d = 1$, Eq. (16) can be solved exactly. A stationary distribution in this case is uniform, as seen in Fig. (1), given by $\rho = (1 - f_A)/L$. Inserting this into Eq. (16) yields a formula for f_A given by

$$f_A = \frac{2}{2 + \lambda}. \quad (18)$$

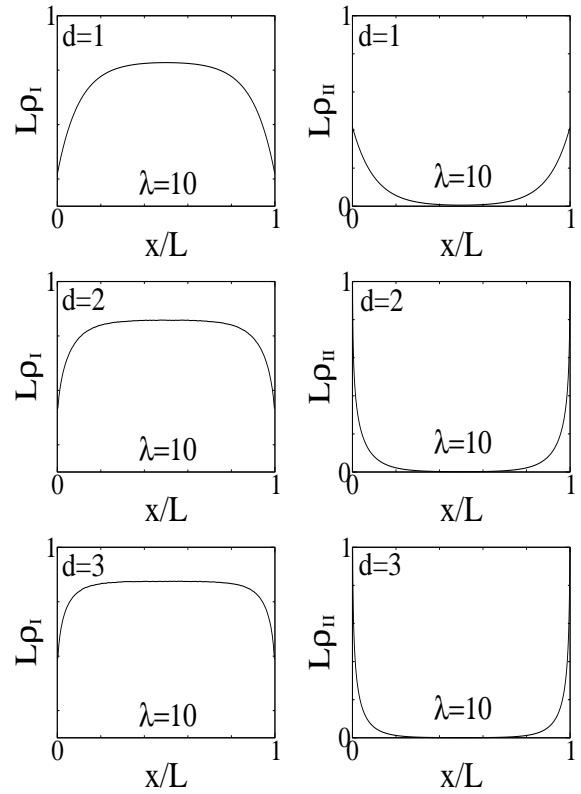


FIG. 2. Contributions to a stationary distributions ρ . ρ_I corresponds to the first line and ρ_{II} corresponds to the second line in Eq. (16). The dimensionless parameter λ is defined as $\lambda = \frac{L}{\tau v_0}$.

VI. ANALOGY WITH THE SPLITTING PROBABILITY PROBLEM

By redefining the RTP motion as a jump process, we inadvertently link the RTP system of particles confined between two walls to the splitting probability problem [4]. The splitting probability $\pi(x)$ is the probability that a particle starting at $x \in [0, L]$ reaches a wall at $x = L$ without first being adsorbed onto a wall at $x = 0$. The splitting probability $\pi(x)$ satisfies the following integral equation [4]

$$\pi(x) = \int_0^L dx' \pi(x') G(x' - x) + \int_L^\infty dx' G(x' - x). \quad (19)$$

The second term in the above equation is the probability of reaching the wall at $x = L$ in a single jump, and the first term is the probability of reaching the same wall in multiple jumps.

To make the analogy between the splitting probability problem and the stationary RTP system more obvious, we differentiate Eq. (19) with respect to x . This leads to

$$\begin{aligned} \frac{d\pi}{dx} = & \int_0^L dx' G(x' - x) \frac{d\pi}{dx'} \\ & + \pi(0)G(x) + [1 - \pi(L)]G(x - L). \end{aligned} \quad (20)$$

Comparing the above equation with Eq. (16), we establish the

following identities:

$$\rho = \frac{d\pi}{dx}, \quad (21)$$

indicating that $\rho(x)$ is the derivate of $\pi(x)$, and the boundary conditions of the probability $\pi(x)$ are found to be related to the fraction of adsorbed particles,

$$\begin{aligned} \pi(0) &= \frac{f_A}{2} \\ \pi(L) &= 1 - \frac{f_A}{2}. \end{aligned} \quad (22)$$

One advantage of Eq. (19) is that $\pi(x)$ does not diverge at the walls. The equality $\pi(0) = f_A/2$ is especially interesting. It tells us that the fraction of adsorbed particles at a wall is the same as the probability of reaching that wall by a particle that initially is adsorbed at another wall, without being re-adsorbed during its random walk.

The reinterpretation of the RTP system as the splitting probability problem, formulated as the integral equation in Eq. (19), together with the relations in Eq. (21) and Eq. (22), is the main result of this work. The important point is that Eq. (19) is not derived from the Fokker-Planck equation but is obtained by changing the microscopic process itself.

Certain properties of $\pi(x)$ can be established from symmetry considerations. For example, for a particle starting from the middle of the interval, the splitting distribution is $\pi(L/2) = 1/2$, since the likelihood of reaching either wall is the same. Another relation from symmetry is $\pi(L/2-x) + \pi(L/2+x) = 1$. Combining the two previous relations we can establish $\frac{1}{L} \int_0^L dx \pi(x) = \frac{1}{2}$, which means that considering all starting points on $(0, L)$, there is on average fifty percent chance that a particle will reach a wall at $x = L$.

The integral in Eq. (19) can be expanded by repetitive elimination of $\pi(x)$ on the right-hand-side with the initial terms of expansion given by

$$\begin{aligned} \pi(x) &= \int_L^\infty dx' G(x-x') \\ &+ \int_0^L dx' G(x-x') \int_L^\infty dx'' G(x'-x'') \\ &+ \int_0^L dx' G(x-x') \int_0^L dx'' G(x'-x'') \int_L^\infty dx''' G(x''-x''') \\ &+ \dots \end{aligned} \quad (23)$$

This allows us to express $\pi(0)$ as $\pi(0) = \sum_{n=1}^\infty p_n$ where p_n is the probability to reach the wall at $x = L$ in n jumps without being re-adsorbed. Explicit expressions for p_n for initial terms is given below

$$\begin{aligned} p_1 &= \int_L^\infty dx' G(x') \\ p_2 &= \int_0^L dx' G(x') \int_L^\infty dx'' G(x'-x'') \\ p_3 &= \int_0^L dx' G(x') \int_0^L dx'' G(x'-x'') \int_L^\infty dx''' G(x''-x'''). \end{aligned} \quad (24)$$

A. the case $d = 1$

Given that for $d = 1$, ρ is uniform and given by $\rho = (1 - f_A)/L$, $\pi(x)$ can be obtained from Eq. (21) and the boundary conditions in Eq. (22), leading to

$$\pi(x) = \frac{1}{2} + (1 - f_A) \left(\frac{x}{L} - \frac{1}{2} \right). \quad (25)$$

Inserting the above expression into Eq. (19) yields

$$\frac{f_A}{2} = \frac{1}{2 + \lambda}, \quad (26)$$

which recovers the result in Eq. (18) and agrees with an alternative derivation based on solving a stationary Fokker-Planck equation [17, 18].

Since the system in $d = 1$ is analytically tractable, we can obtain other exact results. For example, for a particle starting at one of the walls, an expression for the average number of steps needed to reach the opposite wall, defined as

$$\langle n \rangle = \frac{2}{f_A} \sum_{n=1}^\infty n p_n, \quad (27)$$

can be obtained by generating initial terms of the expansion $\langle n \rangle = c_0 + c_1 \lambda + \dots$ and then extracting from those terms a general sequence function. For the exponential distribution G corresponding to $d = 1$ the expansion of p_n starts from

$$p_n(\lambda) = \frac{\lambda^{n-1}}{2^n} + O(\lambda^n). \quad (28)$$

From this it follows that the λ -expansion of $\langle n^k \rangle$ can be represented as

$$\begin{aligned} \frac{f_A}{2} \langle n^k \rangle &= p_1(0) \\ &+ \lambda \lim_{\lambda \rightarrow 0} \left[\frac{dp_1}{d\lambda} + 2^k \frac{dp_2}{d\lambda} \right] \\ &+ \frac{\lambda^2}{2!} \lim_{\lambda \rightarrow 0} \left[\frac{d^2 p_1}{d\lambda^2} + 2^k \frac{d^2 p_2}{d\lambda^2} + 3^k \frac{d^2 p_3}{d\lambda^2} \right] \\ &+ \frac{\lambda^3}{3!} \lim_{\lambda \rightarrow 0} \left[\frac{d^3 p_1}{d\lambda^3} + 2^k \frac{d^3 p_2}{d\lambda^3} + 3^k \frac{d^3 p_3}{d\lambda^3} + 4^k \frac{d^3 p_4}{d\lambda^3} \right] \\ &+ \dots \end{aligned} \quad (29)$$

Based on the initial terms of generated sequences it was possible to determine

$$\langle n \rangle = \frac{1}{6} \frac{12 + 12\lambda + 6\lambda^2 + \lambda^3}{2 + \lambda}, \quad (30)$$

and

$$\langle \Delta n^2 \rangle = \frac{180\lambda + 360\lambda^2 + 240\lambda^3 + 75\lambda^4 + 12\lambda^5 + \lambda^6}{90(\lambda + 2)^2}, \quad (31)$$

where $\Delta n^2 = n^2 - \langle n \rangle^2$.

B. general asymptotic behavior

Analytical formulas derived above for f_A , $\langle n \rangle$, and $\langle \Delta n^2 \rangle$, although corresponding to a specific dimension, can be used to infer an asymptotic behavior for any dimension using assumptions of the central limit theorem. Eq. (26) for $d = 1$ in the limit $\lambda \rightarrow \infty$ yields

$$\frac{f_A}{2} \approx \frac{1}{\lambda}. \quad (32)$$

According to the central limit theorem, after a large number of steps (or jumps as applies to our case), specific details of a distribution G become unimportant and the sole relevant parameter is the standard deviation $\sqrt{\langle \Delta x^2 \rangle}$, which based on Eq. (15) is given by

$$\sigma_d = \tau v_0 \sqrt{\frac{2}{d}}, \quad (33)$$

where the subscript d indicates the dependence on dimension. Consequently, a length scale that is specific to a given dimension is σ_d (rather than τv_0 used previously). This means that the wall separation L when partitioned into segments σ_d will have different dimensionless size,

$$\lambda_d = \frac{L}{\sigma_d} = \lambda \sqrt{\frac{d}{2}}.$$

Based on this, we can redefine the asymptotic formula in Eq. (32) as

$$\frac{f_A}{2} \approx \frac{1}{\sqrt{2}} \frac{1}{\lambda_{d=1}} = \frac{1}{\lambda}.$$

Generalizing the above formula to any d yields

$$\frac{f_A}{2} \approx \frac{1}{\sqrt{2}} \frac{1}{\lambda_d} = \frac{1}{\sqrt{d}} \frac{1}{\lambda}. \quad (34)$$

Following the same procedure, we can generalize the formulas in Eq. (30) and Eq. (31),

$$\langle n \rangle \approx \frac{\lambda^2 d}{6}, \quad \langle \Delta n^2 \rangle \approx \frac{\lambda^4 d^2}{90}. \quad (35)$$

Eq. (34) agrees with the asymptotic behavior obtained using alternative derivation in [4], and which is formulated as

$$\frac{f_A}{2} = \pi(0) \approx \frac{a}{L},$$

where a corresponds to the coefficient of expansion $\tilde{G}(k) = 1 - a^2 k^2 + O(k^4)$, where $\tilde{G}(k) = \int_{-\infty}^{\infty} dl e^{ikl} G(l)$.

C. the case $d = 2$

Analytical results for $d > 1$ are more challenging to derive. The reason can be traced to the presence of a logarithmic singularity in G . For example, the series expansion of p_n in λ

contains logarithmic terms $\ln \lambda$. This makes the computation of p_n from Eq. (24) difficult.

From the initial terms of the series expansion of p_n we get the initial terms of the expansion of f_A ,

$$\begin{aligned} \frac{f_A}{2} &= \frac{1}{2} - \lambda \left(\frac{1}{2\pi} - \frac{\gamma + \ln \frac{\lambda}{2}}{2\pi} \right) \\ &\quad - \lambda^2 \left(\frac{15 - \pi^2}{24\pi^2} - \frac{\gamma + \ln \frac{\lambda}{2}}{4\pi^2} \right) \\ &\quad + \dots, \end{aligned} \quad (36)$$

and the asymptotic behavior in the limit $\lambda \rightarrow \infty$ is determined based on Eq. (34).

D. the case $d = 3$

Following the similar procedure to that for $d = 2$, we get the following initial terms for the expansion of f_A :

$$\begin{aligned} \frac{f_A}{2} &= \frac{1}{2} - \lambda \left(\frac{1}{4} - \frac{\gamma + \ln \lambda}{4} \right) \\ &\quad - \lambda^2 \left(\frac{27 - \pi^2}{96} - \frac{\gamma + \ln \lambda}{16} \right) \\ &\quad + \dots \end{aligned} \quad (37)$$

The asymptotic behavior in the limit $\lambda \rightarrow \infty$ is obtained from Eq. (34).

VII. NUMERICAL SOLUTION

For $d > 1$ where exact results are limited, the integral equation can be solved numerically. To solve Eq. (19), we use an iterative procedure,

$$\pi^{(n+1)}(x) = \int_0^L dx' \pi^{(n)}(x') G(x' - x) + \int_L^\infty dx' G(x' - x), \quad (38)$$

with the initial splitting probability corresponding to $d = 1$ (see Eq. (25)),

$$\pi^{(0)}(x) = \frac{1}{2} + \left(1 - f_A^{(0)}\right) \left(\frac{x}{L} - \frac{1}{2}\right), \quad (39)$$

where $f_A^{(0)} = \frac{2}{2+\lambda}$ according to Eq. (18).

The first iteration can be carried out analytically and the fraction of adsorbed particles for $d = 3$ is found to be

$$f_A^{(1)} = 1 - \frac{\lambda(1 + \lambda\Gamma(0, \lambda) - e^{-\lambda})}{1 + \lambda - e^{-\lambda}}. \quad (40)$$

The above expression is exact up to the second order term in λ . Each subsequent iteration corrects the next higher order term of the expansion of f_A .

In Fig. (3) we plot $\pi(x)$ for $\lambda = 1$ and for different dimensions obtained using the numerical iteration in Eq. (38). To

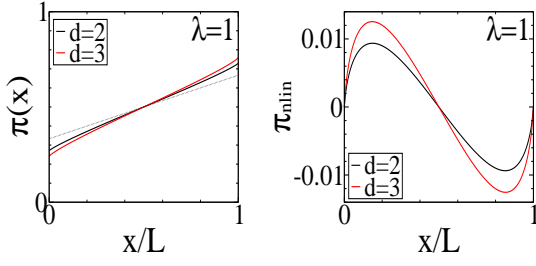


FIG. 3. The splitting probability $\pi(x)$ for $\lambda = 1$ and for dimensions $d = 2$ and $d = 3$. A dashed black line represents $\pi(x)$ for $d = 1$, given in Eq. (25). $\pi^{(n)}$ was found to converge after $n = 10$ iterations. The plots in the figure on the right-hand-side show non-linear contributions of $\pi(x)$.

better highlight the difference of each $\pi(x)$, in Fig. (3) (b) we subtract the linear term from each curve, $\pi_{nlin} = \pi(x) - \pi_{lin}(x)$, where

$$\pi_{lin}(x) = \frac{1}{2} + (1 - f_A) \left(\frac{x}{L} - \frac{1}{2} \right).$$

Since the stationary distribution of RTP particles is given by $\rho = \pi'(x)$, see Eq. (21), from the structure of π_{nlin} we can see how divergences at the walls arise.

VIII. ENTROPY PRODUCTION, DISSIPATION OF HEAT, PRESSURE

A particle moving through a dissipating medium with the velocity \mathbf{v} experiences the frictional force $\mathbf{F}_d = -\mathbf{v}/\mu$. An instantaneous rate of the dissipation of heat is given by $\mathbf{F}_d \cdot \mathbf{v} = \dot{q} = v^2/\mu$. In the case of an unbounded environment, the motion of a RTP particle is unrestricted, thus, the velocity at all times is $|\mathbf{v}| = v_0$ and the average rate of the dissipation of heat (at zero temperature) is

$$\langle \dot{q} \rangle = \frac{v_0^2}{\mu}. \quad (41)$$

For RTP particles confined between two walls, walls start to interfere with the motion (resulting in adsorption), and so not all of the internal energy is converted to heat. The fraction of those particles that are not adsorbed, $1 - f_A$, the heat is dissipated according to Eq. (41). But the motion of adsorbed particles is restricted in the direction perpendicular to the walls, thus, the dissipation of heat of those particles will be reduced. In this case, part of the internal energy that is not converted to heat is manifested as pressure generated by adsorbed particles pushing against the walls.

For a one-dimensional system things are simple. Adsorbed particles are motionless and the heat is dissipated only by particles that are free,

$$\langle \dot{q} \rangle = \frac{v_0^2}{\mu} (1 - f_A). \quad (42)$$

The force exerted on a single wall by adsorbed particles is given by

$$F_p = \frac{v_0}{\mu} \frac{f_A}{2}. \quad (43)$$

For higher dimensions things are more complicated as the motion is restricted only in the direction perpendicular to the walls and particles remain free to move in parallel directions. Thus, to calculate the dissipation of heat, we need to take into account the motion along the wall plane.

In our description we only consider the velocity component perpendicular to the wall, $v \equiv v_\perp$, such that $|v| \leq v_0$. If $\langle \dots \rangle_A$ denotes an average quantity calculated by considering only adsorbed particles, then the dissipation of heat can be defined as

$$\langle \dot{q} \rangle = \frac{v_0^2}{\mu} - \frac{\langle v^2 \rangle_A}{\mu} f_A, \quad (44)$$

where the first term is the dissipation of heat of particles in an unbounded space, and the second term subtracts the heat that is not dissipated due to adsorbed particles with restricted motion.

To calculate $\langle \dot{q} \rangle$, we need to obtain an expression for $\langle v^2 \rangle_A$. Such an expression, within the splitting probability framework, for $\langle v^n \rangle_A$ is given by

$$\begin{aligned} \langle v^n \rangle_A &= \frac{2}{n! \tau^n f_A} \int_0^L dx' \rho(x') \int_L^\infty dx (x-L)^n G(x'-x) \\ &+ \frac{1}{n! \tau^n} \int_L^\infty dx (x-L)^n [G(x-L) + G(x)], \end{aligned} \quad (45)$$

where we used $\langle t_p^n \rangle = n! \tau^n$. The second line represents the probability that a particle becomes re-adsorbed. Eq. (45) can be verified for $d = 1$, in which case $G(x)$ is an exponential function and $\langle v^n \rangle_A = v_0^n$. For $d = 2$ and $d = 3$, the expression is verified by simulations.

From Eq. (44) and Eq. (45) (and using Eq. (21) and Eq. (22)), we get an expression for the dissipation of heat in terms of a splitting probability,

$$\langle \dot{q} \rangle = \frac{v_0^2}{\mu} \frac{d-1}{d} + \frac{2}{\mu \tau^2} \int_0^L dx' \pi(x') \int_L^\infty dx (x-L) G(x-x'). \quad (46)$$

For $d = 1$ the equation above recovers the result in Eq. (42).

It is also possible to obtain an expression for the force acting on a single wall, for a general dimension defined as

$$F_p = \frac{f_A}{2} \frac{\langle v \rangle_A}{\mu}. \quad (47)$$

Using Eq. (45), together with Eq. (21) and Eq. (22), we get

$$F_p = \frac{1}{\tau \mu} \int_0^\infty dx x G(x) - \frac{1}{\tau \mu} \int_0^L dx' \pi(x') \int_L^\infty dx G(x'-x). \quad (48)$$

Once again, we can verify this expression for $d = 1$, which recovers the result in Eq. (43).

In Fig. (4) we plot the fraction particles adsorbed onto a single wall, $f_A/2 = \pi(0)$, and the force exerted on a wall by

those particles, F_p . The results are obtained from $\pi(x)$ calculated numerically and then using the respective formulas. We compare all the results with data points from a simulation based on the Langevin equation.

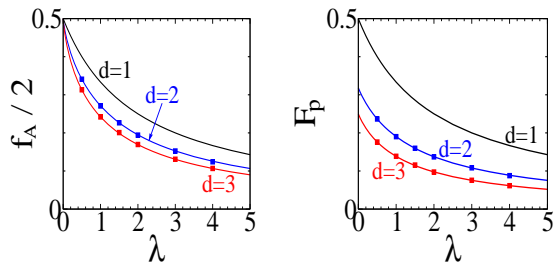


FIG. 4. The fraction of adsorbed particles on a single wall, $f_A/2 = \pi(0)$, and the force exerted by those particles on a single wall, $F_p = f_A \langle v \rangle_A / (2\mu)$, as a function of λ . In the second figure it is assumed that $v_0 = \mu = 1$. The square symbols represent the data points of a dynamic simulation to confirm the numerical results of the splitting probability framework.

The figure shows that adsorption decreases with increasing system dimension. The same trend is observed for the force F_p . At $\lambda = 0$, that is, at the point where the two walls touch one another and all particles are adsorbed, the exerted force increases with decreasing d . This happens because for higher dimensions the probability of motion in the direction parallel to the walls increases.

In Fig. (5) we plot the dissipation of heat (related to the entropy production rate as $T\Pi = \langle \dot{q} \rangle$) as a function of λ . The

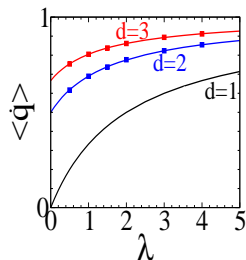


FIG. 5. Dissipation of heat calculated numerically from Eq. (46). It is assumed that $v_0 = \mu = 1$. The square symbols represent the data points of a dynamic simulation based on the Langevin equation.

dissipation of heat increases with increasing d . This again has two causes. The first cause can be traced to the fact that for a lower dimensional system the adsorption is greater, see Fig. (4), and adsorbed particles dissipate less heat. The second cause is that for a larger d , the motion of adsorbed particles is less restricted as there are more available directions along the wall plane. Note that for $\lambda = 0$, where all particles are adsorbed, the dissipation of heat vanishes for $d = 1$. Adsorbed particles in this case are motionless as no parallel motion along the wall is available. In this case all the internal energy is used to generate pressure.

The dissipation of heat for different dimensions can be ac-

curately fit into the following ansatz,

$$\langle \dot{q} \rangle = \frac{v_0^2}{\mu} \left(\frac{d-1}{d} + \frac{1}{d} \frac{\lambda}{c_d + \lambda} \right), \quad (49)$$

with fitting coefficients $c_1 = 2$, $c_2 = 1.63$, $c_3 = 1.4106$ (in the case $d = 1$ the ansatz corresponds to the exact formula). The exact expansion up to the first order term is

$$\langle \dot{q} \rangle = \frac{v_0^2}{\mu} \frac{d-1}{d} + a_d \lambda + \dots \quad (50)$$

with

$$a_d = \frac{1}{2} \frac{\Gamma(d/2)}{\Gamma(1/2)\Gamma(d/2 + 1/2)}.$$

IX. CONCLUSION

The minimal system of RTP particles confined between two walls, despite its apparent simplicity, has not been satisfactorily treated for two- and three-dimensional cases. In this work we treat this system by changing theoretical framework from the Fokker-Planck description to a framework that is consistent with the problem of splitting probability and represented by the integral equation in Eq. (19) together with the relations in Eq. (21) and Eq. (22).

The alternative framework is obtained by modifying the microscopic motion from continuous time dynamics to jump process, in such a way that macroscopic stationary properties of both processes are identical. To do this, it was necessary to determine a correct probability distribution of discontinuous jumps $G(\Delta x)$ that is specific to each dimension, see Eq. (13). For $d = 1$, $G(\Delta x)$ is an exponential function and for the cases $d = 2$ and $d = 3$, $G(\Delta x)$ has a logarithmic singularity at $\Delta x = 0$.

Based on the integral equation it was possible to identify the divergence in the stationary distribution $\rho(x)$ with the probability distributions G positionat at both walls, and representing the distribution of particles recently de-adsorbed.

The integral equation can be solved exactly for the case $d = 1$. The exact treatment of the integral equation for $d = 2$ and $d = 3$ is inhibited by the occurrence of the logarithmic singularity in G . Some limited exact results are possible, such as asymptotic behavior and the initial terms of the expansion of various physical quantities, such as the fraction of adsorbed particles or the dissipation of heat. To solve the integral equation for $\pi(x)$ for those cases, we resort to a numerical iterative scheme.

The procedure to substitute a microscopic process based on continuous dynamics with another process based on discontinuous jumps is not limited or specific to a confinement between walls. At least in principle, it is valid for any other confinement or external potential. The resulting jump algorithm could be a valid alternative to simulations based on the Langevin equation, as long as the focus is on stationary properties.

Appendix A: Jump-algorithm simulation

In this section we compare two simple Python codes for sampling configurations in the interval $x \in [0, L]$. The simulations are specific to $d = 3$, for which the distribution of velocities v is uniform on the interval $[-v_0, v_0]$, see Eq. (5).

The simulation below is based on the numerical integration of the Langevin equation, see Eq. (7). Each step in the simulation corresponds to the next discrete time step $t + dt$. Physical parameters are $v_0 = v_0$, $\tau = \tau$, and $L = L$. A new velocity v is selected from the uniform distribution at the end of a persistence time $t_p = t_p$. A particle is considered as adsorbed when it crosses the location of a wall at $x = 0$ and $x = L$. Once a particle crosses a wall, it is brought to the location of a wall it just crossed.

```
import math
import random
import numpy as np

tau=1 #physical parameters
v0=1
L=1

dt = 0.001 #discrete time interval
NSTEP = 100000 #number of time steps

time=0
tp = np.random.exponential(tau)
v = v0*np.random.uniform(-1,1)
x=0 #initial position
for i in range(0,NSTEP):
    time += dt
    if time>tp: #new velocity selected
        tp = np.random.exponential(tau)
        time=0
        v = v0*np.random.uniform(-1,1)
    x += v*dt
    if x>L: #adsorption onto a wall at x=L
        x=L
```

```
elif x<0: #adsorption onto a wall at x=0
    x=0
```

The Python code below is for a jump-process algorithm. Note that unlike the code above, there is no time variable. Each step corresponds to the next jump. Note that the jump-process algorithm is simpler and more efficiently samples different configurations.

```
import math
import random
import numpy as np

tau=1
v0=1
L=1

NSTEP=10000
x=0
for i in range(0,NSTEP):
    v = v0*np.random.uniform(-1,1)
    tp = np.random.exponential(tau)
    x += tp*v #particle jump
    if x>L:
        x=L
    elif x<0:
        x=0
```

ACKNOWLEDGMENTS

D.F. acknowledges financial support from FONDECYT through grant number 1241694.

Appendix B: DATA AVAILABILITY

The data that support the findings of this study are available from the corresponding author upon reasonable request.

-
- [1] D. Frydel, Positing the problem of stationary distributions of active particles as third-order differential equation, *Phys. Rev. E* **106**, 024121 (2022).
 - [2] M. Caraglio and T. Franosch, Analytic solution of an active brownian particle in a harmonic well, *Phys. Rev. Lett.* **129**, 158001 (2022).
 - [3] D. Frydel, Run-and-tumble oscillator: Moment analysis of stationary distributions, *Physics of Fluids* **35**, 101905 (2023).
 - [4] J. Klinger, R. Voituriez, and O. Bénichou, Splitting probabilities of symmetric jump processes, *Phys. Rev. Lett.* **129**, 140603 (2022).
 - [5] S. N. Majumdar, A. Comtet, and R. M. Ziff, Unified solution of the expected maximum of a discrete time random walk and the discrete flux to a spherical trap, *Journal of Statistical Physics* **122**, 833 (2006).
 - [6] N. G. van Kampen, *Stochastic Processes in Physics and Chemistry* (North-Holland, Amsterdam, 1983).
 - [7] S. Redner, *A Guide to First-Passage Processes* (Cambridge University Press, Cambridge, England, 2001).
 - [8] B. Hughes, *Random Walks and Random Environments* (Oxford University Press, New York, 1995).
 - [9] G. Oshanin and S. Redner, Helix or coil? fate of a melting heteropolymer, *Europhysics Letters* **85**, 10008 (2009).
 - [10] P. Moran, *The Statistical Processes of Evolutionary Theory* (Oxford University Press, New York, 1962).
 - [11] R. Burioni, E. Ubaldi, and A. Vezzani, Superdiffusion and transport in two-dimensional systems with lévy-like quenched disorder, *Phys. Rev. E* **89**, 022135 (2014).
 - [12] Q. Baudouin, R. Pierrat, A. Eloy, E. J. Nunes-Pereira, P.-A. Cuniasse, N. Mercadier, and R. Kaiser, Signatures of lévy flights with annealed disorder, *Phys. Rev. E* **90**, 052114 (2014).
 - [13] M. O. Araújo, T. P. de Silans, and R. Kaiser, Lévy flights of photons with infinite mean free path, *Phys. Rev. E* **103**, L010101 (2021).

- [14] H. C. Berg, *Random Walks in Biology* (Princeton University Press, Princeton, NJ, 1983).
- [15] M. Grognot and K. M. Taute, More than propellers: how flagella shape bacterial motility behaviors, *Current Opinion in Microbiology* **61**, 73 (2021).
- [16] K. Malakar, V. Jemseena, A. Kundu, K. V. Kumar, S. Sabhapandit, S. N. Majumdar, S. Redner, and A. Dhar, Steady state, relaxation and first-passage properties of a run-and-tumble particle in one-dimension, *Journal of Statistical Mechanics: Theory and Experiment* **2018**, 043215 (2018).
- [17] N. Razin, Entropy production of an active particle in a box, *Phys. Rev. E* **102**, 030103 (2020).
- [18] D. Frydel, Intuitive view of entropy production of ideal run-and-tumble particles, *Phys. Rev. E* **105**, 034113 (2022).
- [19] P. Padmanabha, D. M. Busiello, A. Maritan, and D. Gupta, Fluctuations of entropy production of a run-and-tumble particle, *Phys. Rev. E* **107**, 014129 (2023).
- [20] L. Angelani, R. Di Leonardo, and M. Paoluzzi, First-passage time of run-and-tumble particles, *The European Physical Journal E* **37**, 59 (2014).
- [21] F. Mori, P. Le Doussal, S. N. Majumdar, and G. Schehr, Universal survival probability for a d -dimensional run-and-tumble particle, *Phys. Rev. Lett.* **124**, 090603 (2020).
- [22] B. D. Bruyne, S. N. Majumdar, and G. Schehr, Survival probability of a run-and-tumble particle in the presence of a drift, *Journal of Statistical Mechanics: Theory and Experiment* **2021**, 043211 (2021).
- [23] P. Singh and A. Kundu, Local time for run and tumble particle, *Phys. Rev. E* **103**, 042119 (2021).
- [24] U. Basu, S. N. Majumdar, A. Rosso, S. Sabhapandit, and G. Schehr, Exact stationary state of a run-and-tumble particle with three internal states in a harmonic trap, *Journal of Physics A: Mathematical and Theoretical* **53**, 09LT01 (2020).
- [25] D. Frydel, Generalized run-and-tumble model in 1d geometry for an arbitrary distribution of drift velocities, *Journal of Statistical Mechanics: Theory and Experiment* **2021**, 083220 (2021).
- [26] D. Frydel, The run-and-tumble particle model with four-states: Exact solution at zero temperature, *Physics of Fluids* **34**, 027111 (2022), https://pubs.aip.org/aip/pof/article-pdf/doi/10.1063/5.0080058/16644968/027111_1_online.pdf.
- [27] D. Breoni, F. J. Schwarzendahl, R. Blossey, and H. Löwen, A one-dimensional three-state run-and-tumble model with a ‘cell cycle’, *The European Physical Journal E* **45**, 83 (2022).
- [28] J. Tailleur and M. E. Cates, Statistical mechanics of interacting run-and-tumble bacteria, *Phys. Rev. Lett.* **100**, 218103 (2008).
- [29] J. Tailleur and M. E. Cates, Sedimentation, trapping, and rectification of dilute bacteria, *Europhysics Letters* **86**, 60002 (2009).
- [30] N. R. Smith, P. Le Doussal, S. N. Majumdar, and G. Schehr, Exact position distribution of a harmonically confined run-and-tumble particle in two dimensions, *Phys. Rev. E* **106**, 054133 (2022).
- [31] N. R. Smith, P. Le Doussal, S. N. Majumdar, and G. Schehr, Exact position distribution of a harmonically confined run-and-tumble particle in two dimensions, *Phys. Rev. E* **106**, 054133 (2022).
- [32] N. R. Smith and O. Farago, Nonequilibrium steady state for harmonically confined active particles, *Phys. Rev. E* **106**, 054118 (2022).
- [33] A. Dhar, A. Kundu, S. N. Majumdar, S. Sabhapandit, and G. Schehr, Run-and-tumble particle in one-dimensional confining potentials: Steady-state, relaxation, and first-passage properties, *Phys. Rev. E* **99**, 032132 (2019).
- [34] O. Farago and N. R. Smith, Confined run-and-tumble particles with non-markovian tumbling statistics, *Phys. Rev. E* **109**, 044121 (2024).
- [35] C. Roberts and Z. Zhen, Run-and-tumble motion in a linear ratchet potential: Analytic solution, power extraction, and first-passage properties, *Phys. Rev. E* **108**, 014139 (2023).
- [36] P. L. Doussal, S. N. Majumdar, and G. Schehr, Velocity and diffusion constant of an active particle in a one-dimensional force field, *Europhysics Letters* **130**, 40002 (2020).
- [37] T. A. de Pirey and F. van Wijland, A run-and-tumble particle around a spherical obstacle: the steady-state distribution far-from-equilibrium, *Journal of Statistical Mechanics: Theory and Experiment* **2023**, 093202 (2023).
- [38] L. Angelani, Run-and-tumble particles, telegrapher’s equation and absorption problems with partially reflecting boundaries, *Journal of Physics A: Mathematical and Theoretical* **48**, 495003 (2015).
- [39] P. C. Bressloff, Encounter-based model of a run-and-tumble particle ii: absorption at sticky boundaries, *Journal of Statistical Mechanics: Theory and Experiment* **2023**, 043208 (2023).
- [40] E. Woillez, Y. Zhao, Y. Kafri, V. Lecomte, and J. Tailleur, Activated escape of a self-propelled particle from a metastable state, *Phys. Rev. Lett.* **122**, 258001 (2019).
- [41] F. Detcheverry, Non-poissonian run-and-turn motions, *Europhysics Letters* **111**, 60002 (2015).
- [42] D. S. Dean, S. N. Majumdar, and H. Schawe, Position distribution in a generalized run-and-tumble process, *Phys. Rev. E* **103**, 012130 (2021).
- [43] L. Angelani, Confined run-and-tumble swimmers in one dimension, *Journal of Physics A: Mathematical and Theoretical* **50**, 325601 (2017).
- [44] T. Pietrangeli, C. Ybert, C. Cottin-Bizonne, and F. Detcheverry, Optimal run-and-tumble in slit-like confinement, *Phys. Rev. Res.* **6**, 023028 (2024).
- [45] S. C. Takatori, W. Yan, and J. F. Brady, Swim pressure: Stress generation in active matter, *Phys. Rev. Lett.* **113**, 028103 (2014).
- [46] A. P. Solon, Y. Fily, A. Baskaran, M. E. Cates, Y. Kafri, M. Kardar, and J. Tailleur, Pressure is not a state function for generic active fluids, *Nature Physics* **11**, 673 (2015).
- [47] A. P. Solon, J. Stenhammar, R. Wittkowski, M. Kardar, Y. Kafri, M. E. Cates, and J. Tailleur, Pressure and phase equilibria in interacting active brownian spheres, *Phys. Rev. Lett.* **114**, 198301 (2015).
- [48] C. F. Lee, Active particles under confinement: aggregation at the wall and gradient formation inside a channel, *New Journal of Physics* **15**, 055007 (2013).
- [49] C. G. Wagner, M. F. Hagan, and A. Baskaran, Steady-state distributions of ideal active brownian particles under confinement and forcing, *Journal of Statistical Mechanics: Theory and Experiment* **2017**, 043203 (2017).
- [50] D. Frydel, Entropy production of active particles formulated for underdamped dynamics, *Phys. Rev. E* **107**, 014604 (2023).